

Role of Radicals and Singlet Oxygen in Photoactivated DNA Cleavage by the Anticancer Drug Camptothecin: An Electron Paramagnetic Resonance Study

V. Brezova,[†] M. Valko,^{*,†} M. Breza,[†] H. Morris,[‡] J. Telser,[§] D. Dvoranova,[†] K. Kaiserova,[†] L. Varecka,[†] M. Mazur,[†] and D. Leibfritz^{||}

School of Pharmacy and Chemistry, Liverpool John Moores University, Liverpool L3 3AF, United Kingdom, Faculty of Chemical and Food Technology, Slovak Technical University, SK-812 37 Bratislava, Slovakia, Department of Organic Chemistry 2/NW2, Bremen University, D-283 59 Bremen, Germany, and Chemistry Program, Roosevelt University, 430 South Michigan Avenue, Chicago, Illinois 60605

Received: December 17, 2002

Camptothecin (CPT) is an anticancer drug that inhibits topoisomerase I (Topo I), an enzyme closely linked to cell division, by forming a ternary DNA–CPT–Topo I complex. However, it has been shown that UVA-irradiated CPT in the absence of Topo I produces DNA damage. It has been proposed that free radicals are the key species responsible for the DNA cleavage. It has also been shown that the presence of metal ions enhances the activity of several anticancer drugs. Therefore, we attempt here to explore and identify free radicals generated in these processes. We describe a detailed spectroscopic study of UVA-irradiated CPT and the Cu(II)–CPT complex. From the low-temperature EPR spectrum of the Cu(II)–CPT complex, a proximity between the Cu(II) ion and the 20-hydroxy group of the lactone E ring of CPT is proposed. Upon irradiation ($\lambda = 365$ nm) of the Cu(II)–CPT complex in deoxygenated dimethyl sulfoxide (DMSO), the EPR signal of Cu(II) measured in situ at room temperature shows formal first-order exponential decay with a formal half-life of 11 min. By the use of a specific Cu(I) chelating agent, neocuproine, it was shown that, during this process, Cu(II) is reduced to Cu(I). When the photochemical experiments are repeated in oxygen-saturated DMSO solutions, analogous phenomena are observed, characterized by a formal half-life of 16 min for Cu(II), except that there is an induction period of ~ 3 min. Application of the spin-trap agent 5,5-dimethyl-1-pyrroline *N*-oxide (DMPO) shows that during this induction period the only radical formed is the superoxide radical, trapped as the $\cdot\text{DMPO}-\text{O}_2^-$ adduct. The loss in EPR signal intensity of the Cu(II)–CPT complex upon irradiation is accompanied by the appearance of a new EPR signal at $g \approx 2.0022$. Application of the spin traps nitrosodurene (ND) and DMPO revealed that the main radical product formed upon continuous irradiation of CPT in DMSO solutions is the hydroxyl radical (trapped in DMSO as the $\cdot\text{CH}_3$ adduct). Application of 2,2,6,6-tetramethyl-4-piperidinol has revealed that irradiation of CPT in aerated DMSO solution also leads to the formation of singlet oxygen ($^1\text{O}_2$). In the Cu(II)–CPT system, the formation of methyl radicals is suppressed, and the generation of two new radical adducts originating from camptothecin ring cleavage is identified. A mechanism of photochemically generated radicals that include the superoxide radical and the radical cation of the $\{\text{Cu(II)}\cdots\text{CPT}^+\}$ complex followed by the reduction of Cu(II) to Cu(I) is proposed. The EPR experiments on irradiated CPT in the absence of copper (II) support the importance of the 20-hydroxy group of the lactone E ring in the antitumor activity of the drug mediated through the initially generated hydroxyl radical. In the presence of Cu(II), there is blockage of the 20-hydroxy group of CPT, and the generation of hydroxyl radicals is strongly suppressed. In this case, there is a mixture of radicals of various origin generated as a result of irradiation, which are capable of causing DNA damage. We propose that the superoxide radical, hydroxyl radical, singlet oxygen, and carbon-centered radicals generated from CPT in close proximity to DNA can cause considerable damage to DNA. These findings would help to explain the experiments indicating that the photoactivated camptothecin interacts specifically with guanines, consistent with preferential stimulation of topoisomerase I cleavage at sites that bear a guanine at their 5'-DNA terminus. Taken together, our spectroscopic experiments indicate that CPT is a promising photosensitizer and that radicals and singlet oxygen generated upon illumination play a central role in DNA cleavage and in the induction of apoptosis in cancer cells.

Introduction

The anticancer drug camptothecin (CPT) is a plant alkaloid that is very effective in the treatment of gastric, rectum, and bladder tumors.¹ Camptothecin (Figure 1) is a pentacyclic

alkaloid and contains a quinoline ring system (rings A and B), a pyridone ring (ring D), and a terminal α -hydroxy-lactone ring (ring E). From structure–activity studies, it appears that the lactone E ring is essential for antitumor activity. Several clinically important derivatives of CPT have been also synthesized; the most recent involve topotecan (Tpt) and irinotecan.² Topotecan is currently marketed under the tradename Hycamtin for the treatment of ovarian cancer and small-cell lung cancer.

* Corresponding author. E-mail: mvalko@cvt.stuba.sk.

[†] Liverpool John Moores University.

[‡] Slovak Technical University.

^{||} Bremen University.

[§] Roosevelt University.

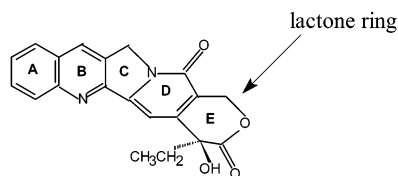


Figure 1. Structure of camptothecin (CPT) (lactone form).

TABLE 1: Comparative Results of DNA Cleavage Mediated by the Anticancer Drug Camptothecin and Its Analogue in the Presence of Topoisomerase I and Irradiation by UVA Light (365 nm)^a

camptothecin and its derivatives	% DNA cleavage with topoisomerase, no irradiation	% DNA cleavage without topoisomerase, with irradiation	
		no Cu(II)	with Cu(II)
none	5.4 ± 1.4	2.5	2.6
camptothecin	66.0 ± 5.1	40	51
20-deoxycamptothecin	4.7 ± 1.5	26	28
10-hydroxycamptothecin	64 ± 6.0	4.2	1.7

^a Results are taken from ref 3d.

The CPT family of drugs appears to have a unique mechanism of action.³ Hertzberg and co-workers discovered that camptothecin inhibits topoisomerase I.^{3d} Topoisomerases are enzymes that control the topological state of DNA in the cell and are required for a number of important DNA processes.⁴ There are two classes of topoisomerases. Type I enzymes regulate DNA under- and overwinding by generating transient single-stranded breaks in the DNA double helix.⁴ Type II enzymes resolve DNA knots and tangles by creating transient double-stranded breaks in the genetic material.⁵

In contrast to the numerous, clinically used drugs targeted to topoisomerase II,⁶ the camptothecin family of drugs appears to be the only compounds currently known that are directed to topoisomerase I. CPT is believed to inhibit topoisomerase I via the formation of a ternary complex in which the biologically active lactone ring of CPT stabilizes an irreversible topoisomerase I/DNA covalent complex.³ The exact structure of the ternary complex is still the subject of intensive investigation.

In the past decade, studies of the possible interaction between CPT or CPT derivatives directly with double-stranded DNA have been reported in the literature.⁷ More than a decade ago, Hertzberg and co-workers,^{3d} Kuwahara and co-workers,^{1v} and more recently Leteurtre et al.^{7c} reported very promising results on DNA cleavage mediated by camptothecin and long-wave UV light in the absence of topoisomerase I.

Results by Hecht and his group^{3d} are presented in Table 1. From this Table, it is evident that camptothecin-mediated DNA cleavage in the presence of light (365 nm) plus copper (II) caused 51% cleaved DNA, a result comparable with the 66 ± 5% camptothecin-mediated DNA cleavage in the presence of topoisomerase I. The experiments by Leteurtre et al.^{7c} have shown that camptothecin-induced DNA cleavage in the presence of light occurred exclusively at guanines at the 5'-DNA terminus, consistent with camptothecin-induced DNA cleavage in the presence of topoisomerase I. Very recent findings, based on time-resolved absorption and emission measurements, confirmed the presence of CPT-induced guanine photolesions.⁸ In addition to these results, Kuwahara et al. claimed that the system of irradiated camptothecin and copper (II) caused phage inactivation.^{1v}

The structure of CPT suggests a basis for its light-mediated DNA cleavage.^{1v,3d,7c} Camptothecin has an extended π -electron system resulting in photosensitive properties; therefore, the

irradiated drug could participate in anticancer action via a free radical mechanism. Radical mechanisms of action have been proposed for several photoactive drugs including bleomycin, actinomycin, hypericin, and mitomycin.⁹ It is also known that some photoactive drugs require the participation of a metal ion for the DNA cleavage event.¹⁰

Taking the above into account, we performed a spectroscopic study of irradiated camptothecin in the presence and absence of copper to explore and identify the radical species generated in these processes. Such a study would help to explain the experimentally observed data by Hertzberg and co-workers^{3d} (Table 1) and others^{1v,7c} indicating DNA cleavage upon irradiation of CPT in the absence of topoisomerase I.

Experimental Section

Chemicals. Camptothecin (Sigma), dimethyl sulfoxide (Fluka, stored over molecular sieves), neocuproine, and CuCl₂·2H₂O (Lachema, Czech Republic) were used without further purification. The spin traps nitrosodurene, 5,5-dimethyl-1-pyrroline *N*-oxide (DMPO), and 2,2,6,6-tetramethyl-4-piperidinol were obtained from Aldrich. DMPO was freshly redistilled before use and stored under argon in a freezer.

EPR Spectroscopy. The EPR spectra at room temperature (290 K) and at 77 K (liquid nitrogen) were measured using a Bruker 200D spectrometer (operating at X band, with 100-kHz field modulation) that was interfaced with an Aspect 2000 computer for data acquisition. The *g* factors were quoted with an uncertainty of ±0.0001 using an internal reference standard marker containing 1,1-diphenyl-2-picrylhydrazyl (DPPH) built into the EPR spectrometer. The simulations of the individual components of the EPR spectra were obtained using the commercially available program SimFonia (Bruker) and the program QPOW developed by Professor Belford, University of Illinois, Urbana, Illinois.¹¹ The complex experimental spin-adduct EPR spectra were then fitted as the linear combinations of these individual simulations using a least-squares minimization procedure with the program Scientist Program (MicroMath). The relative concentrations of the spin adducts were calculated from the contributions of the individual spectra to the experimental spectrum.

In the room-temperature EPR experiments, the freshly prepared solutions were saturated with argon (or oxygen in a special series of experiments) and contained in a quartz cell optimized for the Bruker TM cavity. The samples were irradiated directly in the microwave cavity by monochromatic light ($\lambda = 365$ nm; irradiance 7.3 mW cm⁻²) with a 250-W medium-pressure mercury lamp (Applied Photophysics, England) using a filter (Schott Glaswerke, Germany), and the EPR spectra were monitored *in situ*.

The EPR measurements in liquid nitrogen (77 K) were performed in the standard TE₁₀₂ rectangular cavity using 4-mm o.d. quartz EPR tubes. However, in this case, the solutions were irradiated ($\lambda = 365$ nm) outside of the EPR cavity and immediately frozen in liquid nitrogen, and the low-temperature EPR spectra were then measured. A good-quality amorphous structure was obtained by rapidly cooling the sample in liquid nitrogen. EPR analysis revealed that a complete release of the *g* and A strain had occurred.

Photochemical Steady-State Experiments. In the steady-state photochemical experiments, the samples were irradiated in a quartz cell (0.1-cm path length) with a focused light beam from a 400-W medium-pressure mercury lamp (RWK, Holešovice, Czech Republic) together with an optical filter (Schott Glaswerke, Germany) to select a wavelength of 365 nm. The

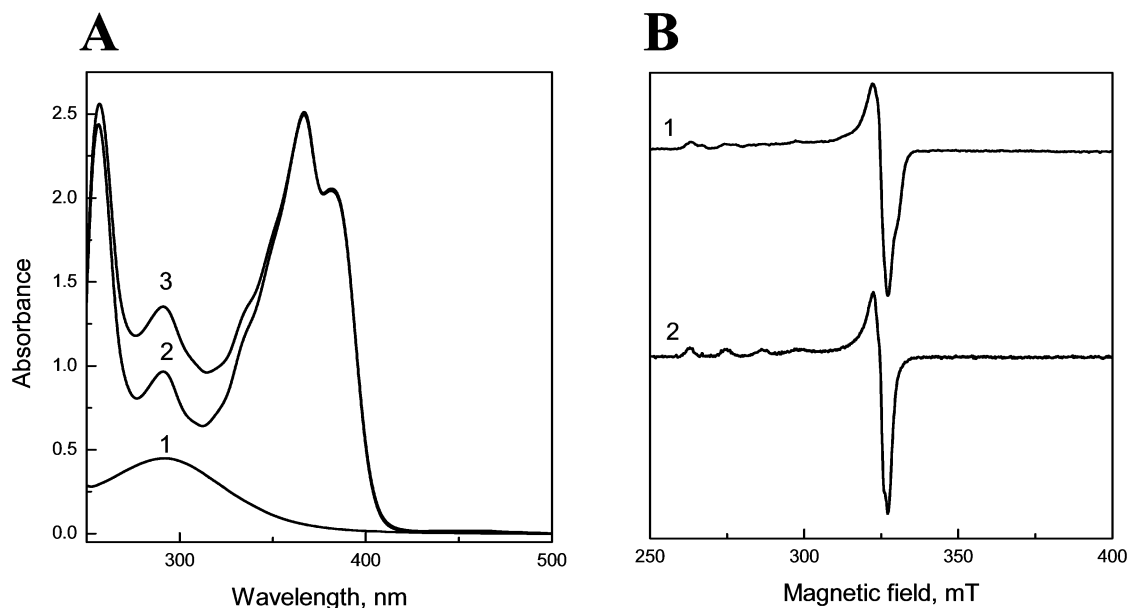


Figure 2. (A) UV/vis spectra of 1 mM DMSO solutions of CuCl₂ (1), CPT (2), and 1:1 Cu(II)–CPT (3). (B) Low-temperature EPR spectra (77 K) of 0.001 M CuCl₂ (1) and 1:1 Cu(II)–CPT (2) in DMSO.

samples were purged with nitrogen for 15 min prior to irradiation. The UV/vis spectra of the irradiated solutions were measured using a UV/vis spectrometer (Philips PU 8800). All steady-state photochemical experiments were performed at room temperature (295 K).

Spectrophotometrical Evidence of Cu(I) Species. The formation of Cu(I) ions upon irradiation was demonstrated spectrophotometrically using the Cu(I) specific chelating agent neocuproine.¹² Solutions of Cu(II)–CPT (0.5 mL) were carefully purged with argon and irradiated at 365 nm in a quartz cell with a path length of 0.2 cm. Neocuproine solutions in DMSO (0.02 M; 0.25 mL) were added, under argon, to the irradiated systems, and after mixing, the absorbance at 458 nm was measured using a diode array UV/vis spectrometer (Ocean Optics, PC 1000). A nonirradiated Cu(II)–CPT sample containing neocuproine was used as a reference.

Results and Discussion

The main intention of this work was to perform a detailed spectroscopic study to identify the key radical species produced by the irradiated Cu(II)–CPT system, which are presumably responsible for the marked DNA cleavage mediated by this system (Table 1). To reveal the effect of light on the Cu(II)–CPT system, we start with the characterization of this complex prior to irradiation. For completeness, results on irradiated CPT in the absence of Cu(II) will also be presented. Because of the very low aqueous solubility of CPT, all of the spectroscopic studies were performed in DMSO solution. DMSO is currently under study as a drug carrier used to increase the effectiveness of some chemotherapy agents for the treatment of some types of cancer; therefore, from a medical point of view, it is an appropriate solvent for these studies.^{1y}

Copper(II)–CPT Complex Prior to Irradiation. To investigate the binding mode of copper to camptothecin, parallel experiments were performed with copper (II) chloride in the absence of the drug. UV/vis spectra of 1 mM DMSO solutions of CuCl₂, CPT, and the 1:1 complex Cu(II)–CPT are shown in Figure 2A. The absorption curve of the Cu(II)–CPT complex may be obtained as a simple linear combination of the corresponding CuCl₂ and CPT individual UV/vis spectra; no

additional charge-transfer bands were observed. The shapes of curves 2 (CPT) and 3 (Cu(II)–CPT) are nearly identical; therefore, it can be concluded that the drug does not bind to copper (II) in the inner coordination sphere. This observation is expected, given that DMSO is a strongly coordinating solvent.

EPR spectroscopy is more useful since this technique is extremely sensitive to the nearest environment around a paramagnetic center (here, Cu(II), 3d⁹, $S = 1/2$).¹³ The low-temperature (77 K) EPR spectrum of CuCl₂ (1 mM) in DMSO is shown in Figure 2B (spectrum 1). The spectrum indicates that the complex is of axial symmetry ($g_{||} = 2.410$, $g_{\perp} = 2.077$, $A_{||} = 11.5$ mT) with all four ^{63,65}Cu ($I = 3/2$) hyperfine transitions in the parallel region resolved.¹³ No hyperfine transitions are resolved in the perpendicular band. This spectrum is that of Cu(II) coordinated by DMSO.¹⁴

The low-temperature EPR spectrum of the Cu(II)–CPT complex (1:1) is also shown in Figure 2B (spectrum 2). At first sight, it appears to be very similar to the spectrum of copper chloride alone; however, careful examination reveals that the perpendicular band is slightly narrower, with a slight rhombic distortion ($g_x = 2.065$, $g_y = 2.090$, $g_z = 2.410$, $A_z = 11.5$ mT) evident. The parallel hyperfine splitting is well resolved with the same hyperfine splitting constant as with Cu(II) alone. The appearance of the EPR spectrum is dependent on the ligands that are directly coordinated to Cu(II).¹³ If the coordinated atom has a nuclear spin, for instance, ¹⁴N ($I = 1$), then an interaction with the electron centered on Cu(II) leads to a splitting of the metal hyperfine lines.¹³ In the case of ¹⁴N donor atoms, the splitting is usually not resolved, and a Cu(II) complex with one or more nitrogen ligands therefore gives rise to rather broad hyperfine lines.^{13a} With ¹⁶O, the naturally abundant isotope has no nuclear spin and does not give rise to hyperfine splitting. A copper (II) complex with only ¹⁶O atoms as ligands may therefore have narrower EPR hyperfine lines. A detailed inspection of the $m_I = -3/2$ parallel line revealed that in the spectra of both CuCl₂ and the Cu(II)–CPT complex a rather narrow parallel hyperfine line ($\Delta B_{||} \approx 2.5$ mT) is observed, suggesting the presence of an oxygen donor set. Therefore, it may be concluded that CPT is weakly coordinated to Cu(II), probably in a second shell through the oxygen atoms of the

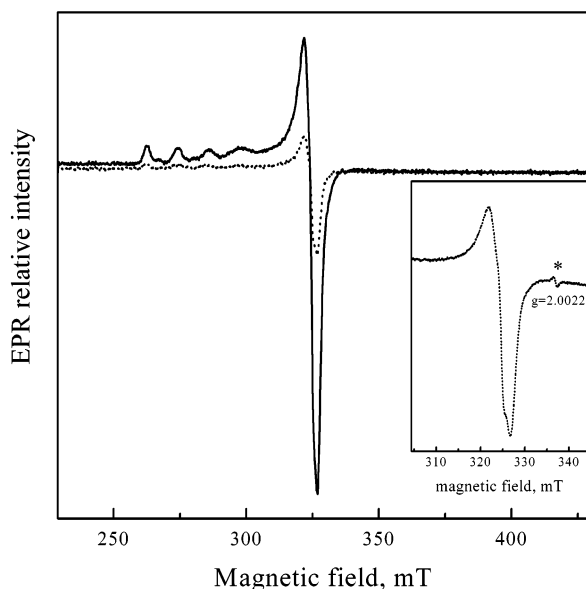


Figure 3. Low-temperature EPR spectra (77 K) of 0.001 M Cu(II)–CPT solution in DMSO before (—) and after 60 min of irradiation at 365 nm (···). The inset expands the spectral region near $g = 2.00$ ($B = 330$ mT), showing the new, radical signal at $g = 2.0022$.

lactone E ring, with DMSO molecules occupying the remaining coordination sites. As presented below, the proximity of the camptothecin E ring and copper is essential for the radical-mediated action of the drug.

Further structural details can be extracted from the EPR spectral data. Correlations between $g_{||}$ and $A_{||}$ (known as P–B diagrams)¹⁵ arise from a variety of factors that have been summarized for natural and artificial copper proteins. It has been well established, particularly for CuX_4 systems, that tetrahedral distortion of a planar CuX_4 moiety markedly reduces $|A_{||}|$ while simultaneously increasing $g_{||}$. The tetrahedral distortion resulting in the dependence of $g_{||}$ on the dihedral angle led to the introduction of the quotient $g_{||}/|A_{||}|$ as a convenient measure of the degree of tetrahedral distortion. The high $g_{||}$ value ($g_{||} = 2.410$) together with the rather small parallel hyperfine splitting constant ($A_{||} = 11.5$ mT) indicates that Cu(II)–CPT in DMSO is a distorted octahedral complex ($g_{||}/|A_{||}| \approx 210$ cm) with only oxygen atoms directly coordinated to the metal ion.

Irradiated Cu(II)–CPT System. We first investigated the EPR properties of irradiated copper chloride in DMSO in the absence of CPT. The EPR signal of irradiated copper chloride in DMSO showed no change in signal intensity with irradiation, indicating that the 2+ oxidation state of copper is extremely stable under these conditions; for example, 30 min of in situ irradiation at 365 nm showed no detectable decrease in the observed EPR intensity.

The presence of CPT causes marked differences in the EPR spectra upon irradiation. The changes in the low-temperature EPR spectra (77 K) of 0.001 M Cu(II)–CPT solution in DMSO before and after 60 min of irradiation at 365 nm under argon are depicted in Figure 3. Irradiation causes a significant reduction in the intensity of the Cu(II) EPR signal: after about 1 h, the intensity is reduced by $\sim 80\%$. This loss of the Cu(II) EPR signal is accompanied by the appearance of a new, weak signal characterized by a g value of 2.0022 (inset in Figure 3). Such a signal is likely “organic” in origin, corresponding to carbon-centered radicals. These radicals were investigated using spin-trapping techniques, as will be described below.

The continuous decrease of the Cu(II) EPR signal upon irradiation was further investigated at room temperature using

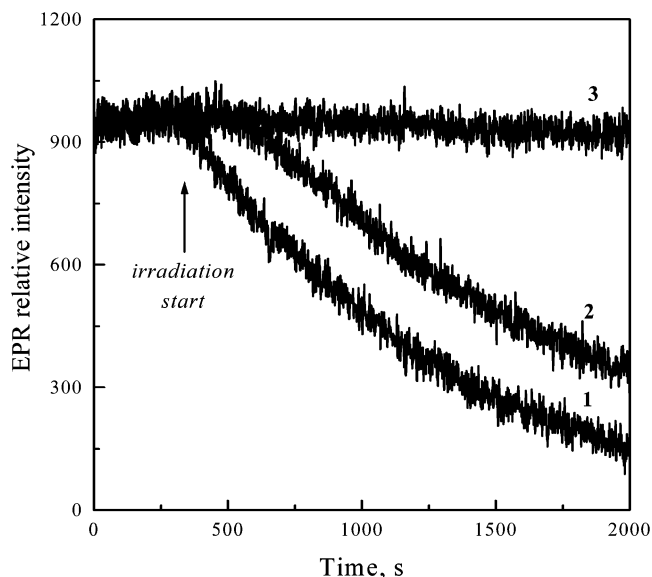


Figure 4. Time dependence of the Cu(II) EPR signal intensity (at $B = 323$ mT) monitored at 290 K upon irradiation of 0.001 M DMSO solutions of (1) 1:1 Cu(II)–CPT under argon, (2) 1:1 Cu(II)–CPT under oxygen, and (3) $CuCl_2$ under argon.

an in situ EPR technique. The magnetic field was locked at the maximum of the Cu(II) EPR signal, and the changes in relative signal intensity as a function of irradiation time were monitored for argon- or oxygen-saturated 1 mM solutions of Cu(II)–CPT in DMSO as well as for the blank, 1 mM $CuCl_2$ in DMSO under argon (Figure 4). It is clear from Figure 4 that there is a substantial decrease in the relative intensity of the Cu(II) EPR signal with time.

The intensity decrease was successfully fitted to an exponential function corresponding to formal first-order kinetics. For the experiments on Cu(II)–CPT in both argon- and oxygen-saturated DMSO solutions, the following points may be noted: (1) For the deaerated Cu(II)–CPT solutions, the decrease in EPR signal intensity starts immediately after irradiation, and the formal half-life of the Cu(II) species is about 11 min. (2) In the presence of oxygen in the Cu(II)–CPT system, there is an initial induction period of about 3 min in which the Cu(II) signal remains constant, after which the species decays at a slightly lower rate (formal half-life of 16 min) as in the deaerated solution. (3) In the absence of CPT, the Cu(II) EPR signal was stable upon in situ irradiation at 365 nm (Figure 4).

The effect of irradiation on the Cu(II)–CPT complex was also investigated by optical spectroscopy. The changes in the UV/vis spectra upon irradiation at 365 nm of a nitrogen-saturated 1 mM solution of Cu(II)–CPT (1:1) in DMSO are depicted in Figure 5. The spectra show an exponential decrease in absorption at 292 nm (Figure 5, inset), which corresponds to the elimination of Cu(II). Despite the slightly different experimental conditions of the steady-state photochemical experiments compared with the in situ EPR technique, the formal half-life from the absorbance measurements evaluated from the band at 292 nm is about 11 min, in good agreement with that determined from the EPR photoexperiments in argon-saturated Cu(II)–CPT solution (Figure 5). The absorbance increase at 415 nm might be interpreted as arising from the photodecomposition of CPT to form products with more extended π -electron systems.

The loss of the EPR signal of the paramagnetic Cu(II) ion upon illumination indicates that this ion is either reduced to Cu(I) ($3d^{10}$) or oxidized to Cu(III) (low-spin $3d^8$). Although Cu(III) is generally considered to be an uncommon oxidation

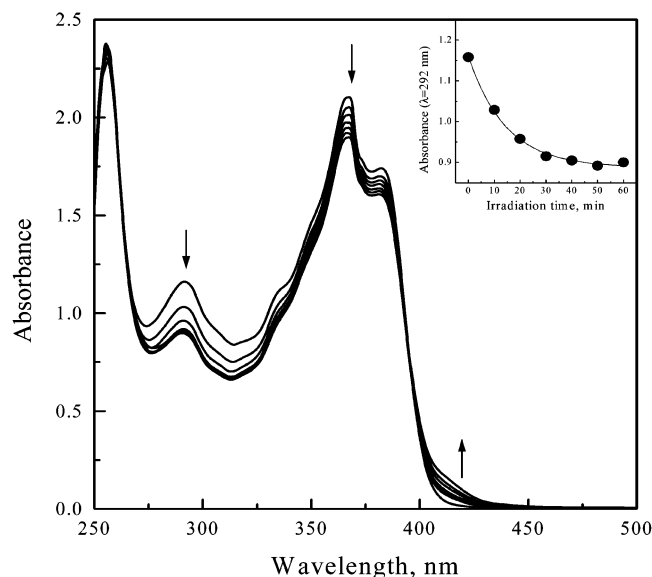


Figure 5. Changes in the UV/vis spectra, measured upon irradiation at 365 nm, of a nitrogen-saturated 1 mM solution Cu(II)–CPT in DMSO. Exposures: 0, 10, 20, 30, 40, 50, and 60 min. Inset: absorbance decrease at $\lambda = 292$ nm monitored during exposure.

state, it is known to occur in reactions relevant to biological processes and consequently cannot be dismissed out of hand.¹⁶ However, Cu(III) is stabilized exclusively in square-planar complexes, and in most of the compounds, sulfur acts as a donor atom.¹⁷ The EPR spectra of Cu(II)–CPT prior to irradiation indicate a distorted octahedral complex, and thus it is unlikely that a square-planar Cu(III) species could be formed; rather, it is likely that Cu(I) is formed.

To obtain direct experimental evidence of the proposed reduction of Cu(II) to Cu(I) upon irradiation of Cu(II)–CPT/DMSO solution, we have employed a specific copper (I) chelator, neocuproine (2,9-dimethyl-1,10-phenanthroline). Neocuproine is a selective chelating agent for Cu(I), forming a colored complex that absorbs at 458 nm.¹² The time evolution of the visible spectra of the irradiated Cu(II)–CPT complex after the addition of neocuproine is depicted in Figure 6 and shows a formal first-order growth with a rate constant of 0.045 min⁻¹. Since the reaction between Cu(I) and neocuproine is fast, this value represents the rate of conversion from Cu(II) to Cu(I) under the given experimental conditions.

Previous studies by Kuwahara et al.^{1v} obtained evidence for the formation of Cu(I) ions in irradiated Cu(II)–CPT solutions. Also relevant are recent investigations of the photochemical formation of Cu(I) from Cu(II)–dicarboxylate complexes, which confirmed that the irradiation of these complexes induces charge transfer and subsequent redox decomposition to Cu(I), carbon dioxide, and various organic products via radical intermediates.¹⁸ It is possible that an analogous mechanism can be invoked here. We thus conclude that irradiation of the Cu(II)–CPT complex leads to the production of Cu(I) and the photodecomposition of CPT,¹⁹ producing radical intermediates.

Formation of Free Radicals. The only way to characterize in detail the radicals produced by the irradiation of the Cu(II)–CPT/DMSO system is to employ an EPR spin-trapping technique. This method involves the trapping of reactive short-lived free radicals by a diamagnetic spin trap compound via an addition reaction to produce a more stable free radical product or spin adduct. The spin adduct that is formed has an EPR spectrum that is characteristic of the type of reactive free radical trapped. Here, we employ the spin traps DMPO and ND

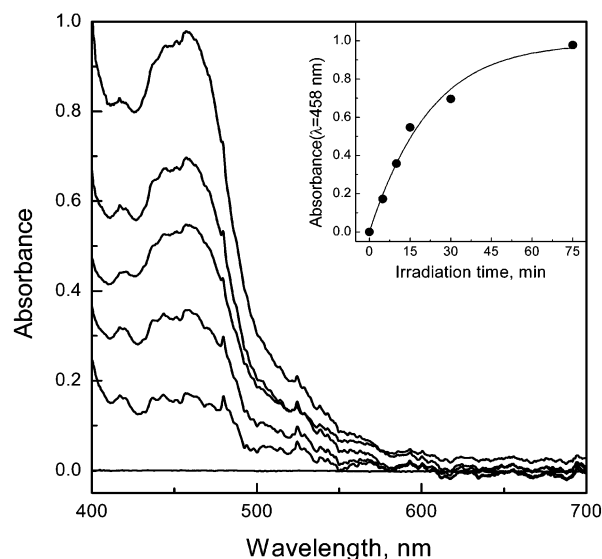
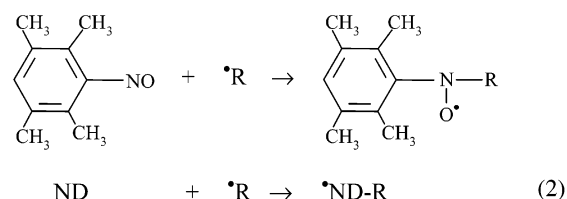
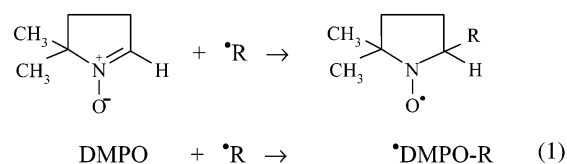


Figure 6. Absorption spectra of irradiated 0.001 M Cu(II)–CPT (1:1) in DMSO after the addition of the Cu(I) specific chelating agent neocuproine. Exposures: 0, 5, 15, 20, 30, and 75 min. Nonirradiated Cu(II)–CPT sample containing neocuproine was used as a reference. Inset: dependence of the Cu(I)–neocuproine characteristic absorbance ($\lambda = 458$ nm) on the irradiation time.

(nitrosodurene).²⁰ DMPO is probably the most widely used spin trap for the study of oxygen-centered free radicals, mainly because of the formation of stable adducts.^{20a,b} The characteristic reactions of DMPO and ND spin traps with radical $\cdot R$ are outlined by eqs 1 and 2.



As documented in Table 1, the most effective DNA cleavage by CPT occurred in the presence of Cu(II). However, we also investigated and analyzed radicals produced in DMSO solution by irradiated CPT in the absence of Cu(II) and by Cu(II) in the absence of CPT.

EPR Spin-Trapping Study of Irradiated and Nonirradiated CPT Alone. Figures 7 and 8 present the set of experimental (solid line) and simulated (dotted line) EPR spectra obtained before and during continuous irradiation at 365 nm of 1 mM DMSO solutions of the CPT (A0 and A1) complex in the presence of ND and DMPO spin traps, respectively. Tables 2 and 3 summarize the EPR parameters obtained from the analysis of the spin adduct spectra for ND and DMPO spin traps, respectively. In the absence of irradiation, no radicals were trapped with either ND or DMPO (Figures 7 and 8-A0). Irradiation of CPT in the presence of ND (Figure 7-A1) yields a single radical with hyperfine coupling constants of $a_N = 1.410$ mT and $a_H(3H) = 1.283$ mT and $g = 2.0055$. This spectrum is assigned to the nitrosodurene–methyl ($\cdot \text{ND-CH}_3$) adduct.²¹ Methyl radicals are produced from the DMSO solvent by its

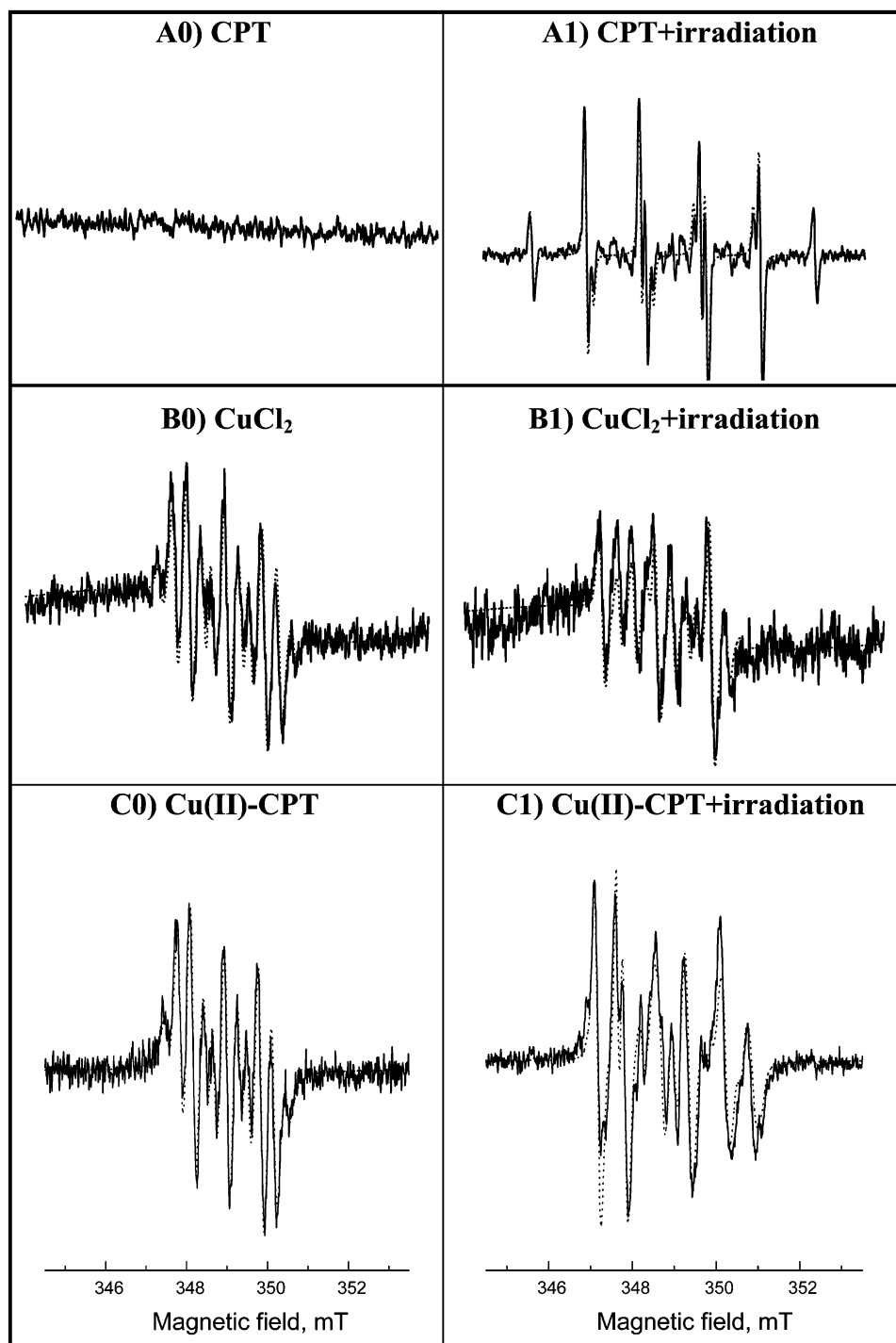
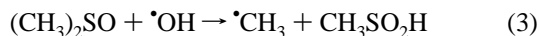


Figure 7. Experimental (—) and simulated (···) EPR spectra obtained in the presence of the ND spin trap before (A0, B0, C0) and upon continuous irradiation at 365 nm under argon (A1, B1, C1) in the 0.001 M DMSO solutions of (A) CPT, (B) CuCl_2 , and (C) Cu(II)-CPT . (Because of the low solubility of the spin trap in DMSO solvent, all solutions were saturated with ND.)

rapid reaction with hydroxyl radicals (the rate constant of the reaction of DMSO with $\cdot\text{OH}$ is $7.0 \times 10^9 \text{ L mol}^{-1} \text{ s}^{-1}$ at 25°C ²²) according to eq 3:



The hydroxyl radicals are most probably released from the lactone ring of CPT.

With DMPO, a more complex spectrum is obtained (Figure 8-A1), which can be interpreted in terms of a six-line pattern corresponding to the methyl radical adduct $\cdot\text{DMPO-CH}_3$ with $a_N = 1.476 \text{ mT}$, $a_H(1\text{H}) = 2.087 \text{ mT}$, and $g = 2.0059$,²¹ upon

which is superimposed a signal with $a_N = 1.300 \text{ mT}$, $a_H(1\text{H}) = 1.49 \text{ mT}$, and $g = 2.0060$, which may be most likely assigned to a $\cdot\text{DMPO-OR}$ adduct,^{21,23} which again originates from the lactone E ring of the drug. Simulation of the complex EPR spectra indicates that the ratio of $\cdot\text{CH}_3$ to $\cdot\text{OR}$ trapped was $\sim 1:2$. Asymmetry in both the extreme low- and high-field lines revealed an additional radical, at low concentration, with the parameters $a_N = 1.410 \text{ mT}$ and $a_H(1\text{H}) = 2.020 \text{ mT}$ and $g = 2.0060$, which is probably a carbon-centered species.^{21,23} Least-squares regression of the experimental spectrum against a sum of the simulated spectra showed the concentration of this third species to be about 5%.

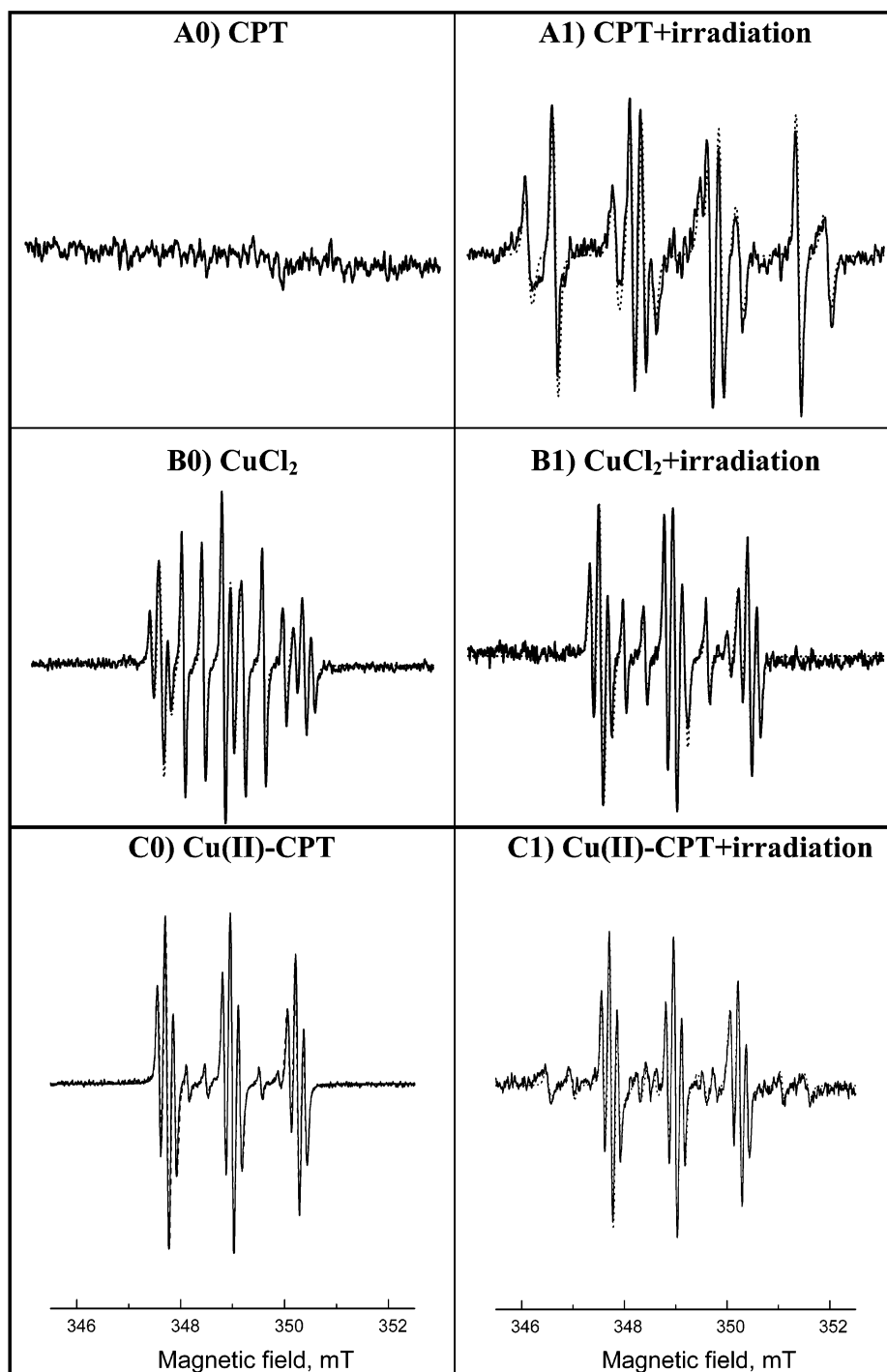


Figure 8. Experimental (—) and simulated (···) EPR spectra obtained in the presence of the DMPO spin trap ($c_{\text{DMPO}} = 0.01$ M) before (A0, B0, C0) and upon continuous irradiation at 365 nm under argon (A1, B1, C1) in the 0.001 M DMSO solutions of (A) CPT, (B) CuCl₂, and (C) Cu(II)–CPT.

In addition to organic radical species formed in photosensitization reactions, singlet oxygen ($^1\text{O}_2$) is known to be produced as well.²⁰ The detection of singlet oxygen is best achieved by the use of 2,2,6,6-tetramethyl-4-piperidinol, which is oxidized to the stable nitroxyl radical, TEMPOL.^{20e–g} The addition of 2,2,6,6-tetramethyl-4-piperidinol to an irradiated aerated solution of CPT yielded the characteristic three-line EPR spectrum of TEMPOL,^{20e–g} as shown in Figure 9A. This result documents that energy transfer from excited CPT to molecular oxygen to form $^1\text{O}_2$ had occurred. No singlet oxygen was detected prior to irradiation.

EPR Spin-Trapping Study of Irradiated and Nonirradiated Cu(II) Alone. Experiments on the Cu(II)–CPT system

using either spin trap are complicated by the reaction of Cu(II) alone with the spin traps. Even in the absence of irradiation, CuCl₂ in DMSO with DMPO produced two radicals (Figure 8-B0), the more abundant (58% of the total) being a nitroxyl radical with $a_{\text{N}} = 1.249$ mT, $a_{\text{H}}(2\text{H}) = 0.147$ mT, and $g = 2.0056$ (an unusually small coupling constant for the β hydrogen). This radical probably arises from the cleavage of the N–C bond and the ring opening of DMPO.²⁴ Superimposed on this signal is a seven-line spectrum with $a_{\text{N}} = 0.699$ mT, $a_{\text{H}}(2\text{H}) = 0.357$ mT, and $g = 2.0065$, which is assigned in the literature to an oxyl radical adduct, $\cdot\text{DMPO-X}$, produced by the oxidation of DMPO.^{21a,24a,25} Similar problems have been reported when DMPO was used in the presence of both

TABLE 2: Simulated EPR Data Obtained in the Presence of the ND Spin Trap before (A0, B0, C0) and upon Continuous Irradiation at 365 nm under Argon (A1, B1, C1) in the 0.001 M DMSO Solutions of (A) CPT, (B) CuCl₂, and (C) Cu(II)–CPT^a

(A0) CPT	(A1) CPT + irradiation
no EPR signals	•ND–CH ₃ $a_N = 1.41$ mT; $a_H(3H) = 1.283$ mT; $g = 2.0055$
(B0) CuCl ₂	(B1) CuCl ₂ + irradiation
•ND–X $a_N = 0.84$ mT, $a_H(3H) = 0.325$ mT; $a_H = 0.31$ mT, $g = 2.0035$ simulation ambiguous	•ND–X 57% •ND–CR ₁ 43% $a_N = 1.1796$ mT; $g = 2.0058$
(C0) Cu(II)–CPT	(C1) Cu(II)–CPT + irradiation
•ND–X	•ND–X 42% •ND–CH ₃ 1% •ND–CR ₂ 8% $a_N = 1.35$ mT; $g = 2.0056$ •ND–CHR ₃ 49% $a_N = 1.525$ mT; $a_H = 0.642$ mT; $g = 2.0055$

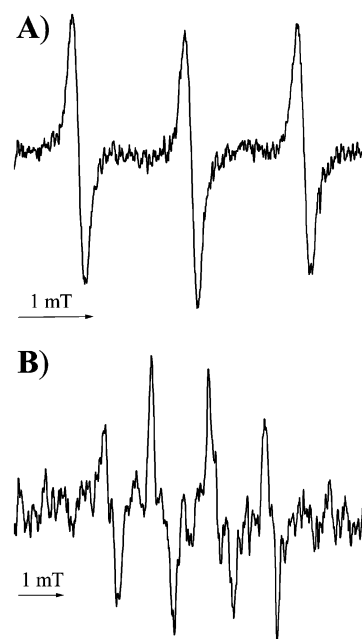
^a See also Figure 7.**TABLE 3: Simulated EPR Data Obtained in the Presence of the DMPO Spin Trap before (A0, B0, C0) and upon Continuous Irradiation at 365 nm under Argon (A1, B1, C1) in the 0.001 M DMSO Solutions of (A) CPT, (B) CuCl₂, and (C) Cu(II)–CPT^a**

(A0) CPT	(A1) CPT + irradiation
no EPR signals	•DMPO–CH ₃ relative concentration 34% $a_N = 1.476$ mT; $a_H = 2.087$ mT; $g = 2.0059$; $a_N/a_H = 0.707$ •DMPO–OR 61% $a_N = 1.30$ mT; $a_H = 1.49$ mT; $g = 2.0060$; $a_N/a_H = 0.872$ •DMPO–CR 5% $a_N = 1.41$ mT; $a_H = 2.02$ mT; $g = 2.0060$; $a_N/a_H = 0.698$
(B0) CuCl ₂	(B1) CuCl ₂ + irradiation
$R_1CH_2C(CH_3)_2N(O^{\bullet})R_2$ $a_N = 1.249$ mT; $a_H(2H) = 0.147$ mT; $g = 2.0056$; $a_N/a_H = 8.497$ 58%	$R_1CH_2C(CH_3)_2N(O^{\bullet})R_2$ 85%
•DMPO–X $a_N = 0.699$ mT; $a_H(2H) = 0.357$ mT; $g = 2.0065$; $a_N/a_H = 1.958$ 42%	•DMPO–X 15%
(C0) Cu(II)–CPT	(C1) Cu(II)–CPT + irradiation
$R_1CH_2C(CH_3)_2N(O^{\bullet})R_2$ 96%	$R_1CH_2C(CH_3)_2N(O^{\bullet})R_2$ 77%
•DMPO–X 4%	•DMPO–X 0.5% •DMPO–CH ₃ 12% •DMPO–OR 10% •DMPO–CR 0.5%

^a See also Figure 8.

cobalt (II)^{25b} and iron(II).²⁶ Irradiation of CuCl₂ in DMSO produced the same two radicals (Figure 8-B1) but in different ratios, viz., 85% of the nitroxyl radical.

Repeating the above experiments with nitrosodurene (Figure 7-B0) gave one radical with $a_N = 0.840$ mT, $a_H(3H) = 0.325$ mT, $a_H(1H) = 0.310$ mT, and $g = 2.0035$ for the nonirradiated system. Irradiated copper chloride (Figure 7-B1) generated an

**Figure 9.** (A) Characteristic EPR spectrum of TEMPOL produced by the oxidation of 2,2,6,6-tetramethyl-4-piperidinol by singlet oxygen: $c_{\text{TEMPO}} = 6$ mM, $c_{\text{CPT}} = 1.8$ mM, irradiation time, 30 s. (B) EPR spectrum of the •DMPO–O₂[–] adduct measured after the 365-nm irradiation of the Cu(II)–CPT oxygen-saturated DMSO solution: $c_{\text{DMPO}} = 0.01$ M, $c_{\text{Cu(II)–CPT}} = 1.0$ mM, irradiation time, 60 s.

additional radical having a three-line spectrum with $a_N = 1.180$ mT and $g = 2.0058$.

EPR Spin-Trapping Study of the Irradiated and Nonirradiated Cu(II)–CPT Complex. As expected, the nonirradiated Cu(II)–CPT system with either spin trap did not produce any new radicals, compared to Cu(II) alone. With DMPO (Figure 8-C0), the only difference was that the ratio of the trapped radicals formed was significantly different: 96:4 for the nitroxyl/oxy radical ratio (cf. 58:42 in the absence of CPT). The presence of CPT seems either to suppress the oxidation reaction or to produce a radical with very similar spin parameters to those of the radical produced from the breakdown of the spin trap.

When the above experiment is repeated with irradiation (Figure 8-C1), the same radicals are produced as in the individual camptothecin and Cu(II) irradiation experiments (Figure 8-A1 and B1, respectively). The nitroxyl/oxy radical ratio is reduced relative to that observed in the reaction between Cu(II) alone and DMPO, and the amount of •OR produced is also reduced from about 61 to 10%, and that of •CH₃, from 34 to 12%. Thus, the presence of Cu(II) appears to inhibit the release of the hydroxyl group from camptothecin, as monitored by the formation of methyl radicals.

The use of DMPO with the irradiated Cu–CPT complex gives evidence only for the superposition of the multicomponent spectra of radicals detected in the separate systems, irradiated CPT and irradiated Cu(II) alone (see Table 2). However, ND has been proven to be a more sensitive spin trap when applied to the irradiated Cu–CPT complex and provides evidence that two additional radicals are generated (Figure 7-C1, Table 2 C1). The less abundant (8%) is carbon-centered and is seen as a triplet with $a_N = 1.35$ mT and $g = 2.0056$.^{21j} The more abundant (49%) radical is seen as a sextet with $a_N = 1.525$ mT, $a_H(1H) = 0.642$ mT, and $g = 2.0055$. The more abundant radical likely originates from the cleavage of the CPT ring since the coupling

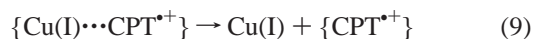
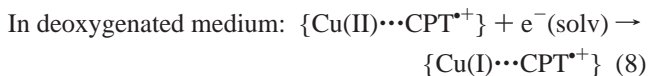
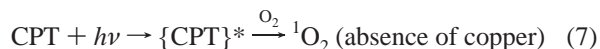
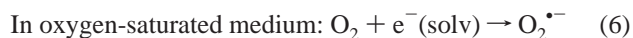
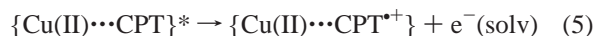
parameters are in good agreement with a spin adduct of the type $(\bullet\text{ND})\text{---CHR=CHR}'$.^{21a,21j} Interestingly, the generation of the $\bullet\text{ND-CH}_3$ adduct in this experiment was strongly suppressed, as this radical adduct represents only 1% of the total signal area. These results support the proposal derived from the EPR spectra that the hydroxyl group of the CPT E ring is bound to Cu(II) or at least is in its proximity. We also note that the blockage of the hydroxyl group of the CPT ring has a significant effect on CPT biological activity, as will be discussed below.

Generation of the Superoxide Ion upon Irradiation of the Aerated Cu(II)–CPT Complex. In contrast to deaerated solutions, where the Cu(II) EPR signal starts to decay immediately after irradiation, aerated solutions exhibit a plateau lasting about 3 min before the decay of the Cu(II) signal (Figure 5). During this period, photoexcited CPT may more easily eject and subsequently transfer an electron to dioxygen, forming superoxide, which is trapped by DMPO. The EPR spectrum of $\bullet\text{DMPO-O}_2^-$ is shown in Figure 9B ($a_N = 1.295$ mT, $a_H = 1.035$ mT, $a_H' = 0.130$ mT, $g = 2.0055$).^{21a,27} During this induction period, while dioxygen is being consumed and superoxide is generated, the Cu(II) signal stays unchanged because the reduction process to Cu(I) cannot take place until all of the dioxygen has been consumed. After this period, the Cu(II) EPR signal starts to decay with a slightly lower rate than in the argon-saturated solution. The experimental EPR spectrum of $\bullet\text{DMPO-O}_2^-$ is slightly noisy because of the short lifetime of $\bullet\text{DMPO-O}_2^-$ under the given experimental conditions, so we were unable to signal average the spectra. However, computer simulation and EPR data are in good agreement with the data reported previously for the $\bullet\text{DMPO-O}_2^-$ adduct.^{21a,27} Upon prolonged irradiation (after oxygen consumption), the same radical adducts are observed in these aerated solutions as in the corresponding argon-saturated solutions (Figure 8-C1).

Possible Photochemical Pathways. It is known that excited species of a phototherapeutic agent can undergo various reactions, among which electron-transfer (ET) and energy-transfer processes are possibly the most important.²⁸ CPT has an extended π -electron system and consequently is photoactive.^{1v,3d,7c} Studies on electron transfer in biochemistry show that, in most cases, direct contact or proximity of the donor and acceptor molecules is necessary for efficient electron transfer, particularly in photoinduced electron transfer.²⁸ For the Cu(II)–CPT system, on the basis of UV/vis and EPR evidence, the proximity between the Cu(II) ion and the CPT molecule has been demonstrated. Thus, we propose that the irradiation of CPT leads to the release of an electron, which is then trapped as a “solvated electron”, accompanied by the formation of the solvated $\{\text{Cu(II)}\cdots\text{CPT}^{\bullet+}\}$ complex. Support for the model that the solvated electron originates from photoexcited CPT can be found in Figure 5 (curve 3), wherein the Cu(II) EPR signal in DMSO absent CPT remains unchanged upon irradiation. This process of electron transfer is particularly efficient in DMSO since it is a highly dipolar, aprotic solvent characterized by the ability to solvate cations strongly but only weakly solvate anions. Thus, DMSO stabilizes the cation radical of CPT, which is an initiator of subsequent radical products (Figure 7-C1).

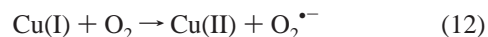
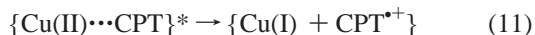
In deoxygenated solution, Cu(II) is immediately reduced to Cu(I), as manifest by the decrease of the copper (II) EPR signal. (See Figure 5, curve 1.) In oxygen-saturated solution, however, there is a period of 3 min during which the solvated electron interacts with dioxygen, forming the superoxide radical (detected by EPR, Figure 9B), and the Cu(II) EPR signal remains unchanged (see Figure 4 and note the induction period of curve 2).

The reaction scheme of radical and singlet oxygen generation can thus be described as follows:



This scheme is in agreement with the proposal that photogenerated, reactive radical products play a significant role in causing single-strand breaks in DNA.^{1v,3d,7c}

We note that we since have no direct evidence for the formation of the solvated electron an alternative mechanism for eqns 5–9 could be



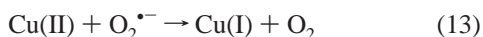
Whichever mechanism prevails does not affect the following arguments.

Biological Implications of Light-Mediated Anticancer Activity of CPT and Cu(II)–CPT. On the basis of our EPR spin-trapping experiments on irradiated CPT, we conclude that hydroxyl radicals are produced, originating from the 20-OH group of CPT. Hydroxyl radicals so generated would most probably be responsible for DNA cleavage. The importance of the 20-hydroxy group in light-mediated cleavage in the absence of topoisomerase I (see Table 1) agrees with the previously demonstrated importance of this group in the topoisomerase I-mediated antitumor activity of CPT.^{3d,19}

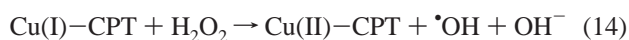
The pioneering work of Hertzberg et al.^{3d} and Huwahara et al.^{1v} also showed the effect of the presence of Cu(II), as the addition of this ion resulted in a further increase in DNA damage (by more than 10%; see Table 1). From the low-temperature EPR data of the Cu(II)–CPT complex, we conclude that the 20-hydroxy group of CPT is involved in binding to Cu(II) or at least is in proximity to the metal. This would protect the 20-hydroxy group, which would inhibit the number of hydroxyl radicals generated. Computer analysis of the multicomponent EPR spectra revealed that Cu(II) indeed suppressed the formation of hydroxyl radicals (trapped in DMSO solvent as $\bullet\text{ND-CH}_3$, Figure 7-C1). Thus, the enhanced DNA cleavage caused by irradiated CPT in the presence of Cu(II) must arise through the formation of radicals produced by photolysis, other than hydroxyl radicals. The studies using the ND spin trap indeed gave evidence for the formation of other radicals.

One of the most striking results was the spin-trapping EPR detection of singlet oxygen (Figure 9A) upon irradiation of aerated CPT solution. Since singlet oxygen is known to be a considerable source of biological damage, in particular to DNA, it can be proposed that this reactive form of oxygen significantly participates in DNA cleavage.

Our EPR study of the irradiated aerated Cu(II)–CPT complex indicated the formation of the superoxide radical anion. Superoxide generated *in vivo* has only moderate biological activity, mainly because of its negative charge, so it can only very slowly cross biological membranes unless there is an anion channel available.²⁹ Nevertheless, chemical, enzymatic, or phagocytic generation of the superoxide radical has been observed to cause considerable biological damage.²⁹ If the Cu(II)–CPT complex in aqueous solution were irradiated in the presence of DNA, then superoxide generated in close proximity to DNA might be converted spontaneously or enzymatically to hydrogen peroxide by dismutation. The latter oxidizing agent would then be able to migrate within the cells and generate the hydroxyl radical. In addition, superoxide $O_2^{\bullet-}$ can efficiently reduce Cu(II) to Cu(I):



Both *in vitro* and *in vivo* studies have shown that the presence of transition-metal ions in their reduced forms (Fe(II), Cu(I)) catalyze the decomposition of naturally generated H_2O_2 within cells, resulting in the production of oxidative radicals.^{29,30} This is known as the Fenton reaction and represents an alternative source of reactive hydroxyl radicals. A version of the Fenton reaction adapted to the current situation is as follows:



This additional mechanism for DNA damage by the copper–CPT system is supported by recent studies that revealed that Cu(II) with H_2O_2 caused DNA base damage.³⁰

The free radical-induced damage to cancer cells currently forms the basis of one of the most active fields of research in applied photochemistry, called tumor phototherapy or photodynamic therapy (PDT).³¹ A drug photosensitizer, which exhibits some selectivity for tumor tissue, is administered, followed by irradiation with UV/vis or near-IR light using fiber optics and laser sources. The excited photosensitizer undergoes various reactions, among which electron transfer and energy transfer are the most important. Free radicals or singlet oxygen produced in these processes are the species mostly responsible for the photonecrosis and damage to cancer cells.³² The properties of irradiated CPT in the presence of Cu(II) described in this work predispose it for testing as a potential candidate for photodynamic therapy.

Conclusions

This work was undertaken to explain the origin of radical species that are responsible for DNA cleavage mediated by CPT in the presence of light. The results can be summarized as follows.

(1) From the low-temperature EPR spectra of the Cu(II)–CPT complex in DMSO solution, we conclude that the hydroxyl group of the CPT E ring is bound to the copper (II) atom or at least stays in proximity to it. The remaining coordination sites of Cu(II) are occupied by DMSO solvent. One hour of UVA ($\lambda = 365$ nm) irradiation of the Cu(II)–CPT complex causes an ~80% reduction in the Cu(II) EPR signal intensity. By the use of a specific Cu(I) chelating agent, neocuproine, it was shown that Cu(II) is reduced to Cu(I). This process is accompanied by the formation of a new EPR signal of organic origin characterized with g value of 2.0022.

(2) To understand better the origin of this weak EPR signal from an organic radical, spin-trapping experiments using DMPO and nitrosodurene were performed. These studies on irradiated

CPT and the irradiated Cu(II)–CPT complex in DMSO confirmed the generation of a variety of transient free radicals. Irradiated CPT in the absence of Cu(II) showed the initial generation of the hydroxyl radical. This highlights the importance of the 20-hydroxy group in lactone ring E for the antitumor activity of CPT. In the presence of Cu(II), there is a blockage of the 20-hydroxy group of CPT, which is involved in copper (II) binding, and the generation of hydroxyl radicals is strongly suppressed. In this case, a number of other radicals, which are themselves capable of causing DNA damage, are generated as a result of irradiation. Another important finding in view of the possible biological consequences (DNA damage to cancer cells) is the formation of singlet oxygen (1O_2) upon the illumination of CPT. A possible photochemical pathway that may include electron solvation immediately followed by the formation of a solvated $\{Cu(II)\cdots CPT^{\bullet+}\}$ complex and then the reduction of Cu(II) to Cu(I) is proposed. In oxygen-saturated solution, spin trapping detected the superoxide radical.

(3) Irradiation of the Cu(II)–CPT complex generates the hydroxyl radical, carbon-centered radicals, and, when dioxygen is present, the superoxide radical. This finding, combined with the growing body of evidence that CPTs may directly interact with DNA, leads us to propose that CPT in the presence of light and Cu(II) cause DNA damage by the direct production of reactive radicals in close proximity to DNA. Our results thus help to explain previously published experiments^{1v,3d,7c} (see also Table 1) involving DNA cleavage mediated by CPT in the presence of light and Cu(II). Our findings also suggest that the properties of photoexcited CPT in the presence/absence of Cu(II) predispose it for testing as a potential candidate for photodynamic therapy.

Acknowledgment. We thank the Grant Agency for financial support (projects VEGA 1/9256/02, VEGA 1/7313/20, and VEGA 1/9255/02) and NATO for a collaborative linkage grant LST.CLG.977743 (to H.M., J.T., and M.V.). We also thank Professor J. Šima, D.Sc. for the gift of neocuproine and Professor G. Stochel, D.Sc. (Jagiellonian University, Krakow, Poland) for fruitful discussions. This paper is dedicated to our colleague and friend, Professor Peter Pelikán, deceased on May 18, 2002.

References and Notes

- (1) (a) Arimondo, P. B.; Bourtoune, A.; Baldeyrou, B.; Bailly, C.; Kuwahara, M.; Hecht, S. M.; Sun, J. S.; Garestier, T.; Helene, C. *J. Biol. Chem.* **2002**, *277*, 3132. (b) Hecht, S. M. *Ann. N.Y. Acad. Sci.* **2000**, *922*, 76. (c) Wang, X. Y.; Zou X. A.; Hecht, S. M. *Biochemistry* **1999**, *38*, 4374. (d) Wang, X. Y.; Short, G. F.; Kingsbury, W. D.; Johnson, R. K.; Hecht, S. M. *Chem. Res. Toxicol.* **1998**, *11*, 1352. (e) Wang, X. Y.; Wang, L. K.; Kingsbury, W. D.; Johnson, R. K.; Hecht, S. M. *Biochemistry* **1998**, *37*, 9399. (f) Wang, L. K.; Rogers, B. D.; Hecht, S. M. *Chem. Res. Toxicol.* **1996**, *9*, 75. (g) Wang, L. K.; Johnson, R. K.; Hecht, S. M. *Chem. Res. Toxicol.* **1993**, *6*, 813. (h) Wall, M. E.; Wani, M. C.; Cook, C. E.; Palmer, K. H.; McPhail, A. T.; Sim, G. A. *J. Am. Chem. Soc.* **1966**, *88*, 3888. (i) *Camptothecins: New Anticancer Agents*; Potmesil, M.; Pinedo, H., Eds.; CRC Press: Boca Raton, FL, 1995. (j) Fan, Y.; Shi, L. M.; Kohn, K. W.; Pommier, Y.; Weinstein, J. N. *J. Med. Chem.* **2001**, *44*, 3254. (k) Wani, M. C.; Nicholas, A. W.; Manikumar, G.; Wall, M. E. *J. Med. Chem.* **1987**, *30*, 1774. (l) Burke, T. G.; Staubus, A. E.; Mishra, A. K. *J. Am. Chem. Soc.* **1992**, *114*, 8318. (m) Burke, T. G.; Mishra, A. K.; Wani, M. C.; Wall, M. E. *Biochemistry* **1993**, *32*, 5352. (n) Mi, Z.; Burke, T. G. *Biochemistry* **1994**, *33*, 10325. (o) Mi, Z.; Burke, T. G. *Biochemistry* **1994**, *33*, 12540. (p) Dey, J.; Warner, I. M. *J. Photochem. Photobiol., A* **1996**, *101*, 21. (r) Chourpa, I.; Millot, J.-M.; Sockalingum, G. D.; Riou, J.-F.; Manfait, M. *Biochim. Biophys. Acta* **1998**, *1379*, 353. (s) Lerchen, H.-G. *Drugs* **1999**, *2*, 896. (t) Koshkina, N. V.; Gilbert, B. E.; Waldrep, J. C.; Seryshev, A.; Knight, V. *Cancer Chemother. Pharmacol.* **1999**, *44*, 187. (u) Pourquier, P.; Pommier, Y. *Adv. Cancer Res.* **2000**, *80*, 189. (v) Kuwahara, J.; Suzuki, T.; Funakoshi, K.; Sugiura, Y. *Biochemistry* **1986**, *25*, 1216. (y) <http://www.cancer.org>. American Cancer Society.
- (2) (a) Burk, P. L.; Fortunak, J. M.; Mellinger, M.; Wood, J. L. *Abstr. Pap. - Am. Chem. Soc.* **1995**, *210*, 135. (b) Henegar, K. E.; Ashford, S.

- W.; Baughman, T. A.; Sih, J. C.; Gu, R. L. *J. Org. Chem.* **1997**, *62*, 6588–6597. (c) Curran, D. P.; Ko, S. B.; Josien, H. *Angew. Chem., Int. Ed. Engl.* **1996**, *34*, 2683. (d) Morales, C.; Zurita, M.; Vaquero, J. *J. Neuro-Oncol.* **2002**, *56*, 219. (e) Houghton, P. J.; Santana, V. M. *J. Pediatr. Hematol. Oncol.* **2002**, *24*, 84.
- (3) (a) Hsiang, Y.-H.; Hertzberg, R.; Hecht, S.; Liu, L. F. *J. Biol. Chem.* **1985**, *260*, 14873. (b) Mattern, M. R.; Mong, S.-M.; Bartus, H. F.; Mirabelli, C. K.; Crooke, S. T.; Johnson, R. K. *Cancer Res.* **1987**, *47*, 1793. (c) Hsiang, Y.-H.; Liu, L. F. *Cancer Res.* **1988**, *48*, 1722. (d) Hertzberg, R. P.; Caranfa, M. J.; Hecht, S. M. *Biochemistry* **1989**, *28*, 4629. (e) Liu, L. F. *Camptothecins: New Anticancer Agents*; Potmesil, M., Pinedo, H., Eds.; CRC Press: Boca Raton, FL, 1995; p 9.
- (4) (a) Sobhani, A. M.; Ebrahimi, S. A.; Mahmoudian, M. *J. Pharm. Pharm. Sci.* **2002**, *5*, 19. (b) Christensen, M. O.; Barthelmes, H. U.; Feineis, S.; Knudsen, B. R.; Andersen, A. H.; Boege, F.; Mielke, C. *J. Biol. Chem.* **2002**, *277*, 15661.
- (5) (a) Kimura, K.; Rybenkov, V. V.; Crisona, N. J.; Hirano, T.; Cozzarelli, N. R. *Cell* **1999**, *98*, 239. (b) Hartsuiker, E.; Bahler, J.; Kohli, J. *Mol. Biol.* **1998**, *9*, 2739. (c) Rodriguez-Campos, A. *J. Biol. Chem.* **1996**, *271*, 14150.
- (6) (a) Beck, W. T.; Morgan, S. E.; Mo, Y. Y.; Bhat, U. G. *Drug Resist. Updates* **1999**, *2*, 382. (b) Lee, K. H. *Med. Res. Review* **1999**, *19*, 569. (c) Kim, R.; Tanabe, K.; Uchida, Y.; Osaki, A.; Toge, T. *Oncol. Reports* **2002**, *9*, 3.
- (7) (a) Yang, D.; Strobe, J. T.; Spelmann, H. P.; Wang, A. H.-G.; Burke, T. G. *J. Am. Chem. Soc.* **1998**, *120*, 2979. (b) Streltsov, S.; Sukhanova, A.; Mikheikin, A.; Grokhovsky, S.; Zhuze, A.; Kudelina, I.; Mochalov, K.; Oleinikov, V.; Jardillier, J. C.; Nabiev, I. *J. Phys. Chem. B* **2001**, *105*, 9643. (c) Leteurtre, F.; Fesen, M.; Kohlhaagen, G.; Kohn, K. W.; Pommier, Y. *Biochemistry* **1993**, *32*, 8955. (d) Fan, Y.; Weinstein, J. N.; Kohn, K. W.; Shi, L. M.; Pommier, Y. *J. Med. Chem.* **1998**, *41*, 2216. (e) Streltsov, S. A.; Grokhovskii, S. L.; Kudelina, I. A.; Oleinikov, V. A.; Zhuze, A. L. *Mol. Biol.* **2001**, *35*, 365.
- (8) Steenkeste, K.; Guiot, E.; Tfibel, F.; Pernot, P.; Merola, F.; Georges, P.; Fontaine-Aupart, M. P. *Chem. Phys.* **2002**, *275*, 93.
- (9) Bleomycin: (a) Quada, J. C.; Boturyn, D.; Hecht, S. M. *Bioorg. Med. Chem.* **2001**, *9*, 2303. (b) Kane, S. A.; Sasaki, H.; Hecht, S. M. *J. Am. Chem. Soc.* **1995**, *117*, 9107. (c) Natrajan, A.; Hecht, S. M. *J. Org. Chem.* **1991**, *56*, 5239. (d) Fattman, C. L.; Chu, C. T.; Kulich, S. M.; Enghild, J. J.; Oury, T. D. *Free Radical Biol. Med.* **2001**, *31*, 1198. (e) Childs, A.; Jacobs, C.; Kaminski, T.; Halliwell, B.; Leeuwenburgh, C. *Free Radical Biol. Med.* **2001**, *31*, 745. Actinomycin: (f) Pan, J.-X.; Liu, Y.; Zhang, S.-P.; Tu, T.-C.; Yao, S.-D.; Lin, N.-Y. *Biochim. Biophys. Acta* **2001**, *1527*, 1. (g) Schulz, J. B.; Bremen, D.; Reed, J. C.; Lommatzsch, J.; Takayama, S.; Wullner, U.; Loschmann, P. A.; Klockgether, T.; Weller, M. *J. Neurochem.* **1997**, *69*, 2075. Hypericin: (h) Falk, H. *Angew. Chem., Int. Ed.* **1999**, *38*, 3117. Mirossay, A.; Onderkova, H.; Mirossay, L.; Sarissky, M.; Mojzis, J. *Physiol. Res.* **2001**, *50*, 635. Mitomycin: (j) Kammerer, C.; Getoff, N. *Radiat. Phys. Chem.* **2001**, *61*, 35. (k) Yamagishi, M.; Osakabe, N.; Natsume, M.; Adachi, T.; Takizawa, T.; Kumon, H.; Osawa, T. *Food Chem. Toxicol.* **2001**, *39*, 1279.
- (10) (a) McMillin, D. R.; McNett, K. M. *Chem. Rev.* **1998**, *98*, 1201. (b) Lugo-Ponce P.; McMillin, D. R. *Coord. Chem. Rev.* **2000**, *208*, 169. (c) Ou, Z. Z.; Chen, J. B.; Wang, X. S.; Zhang, B. W.; Cao, Y. *Chem. Lett.* **2002**, *2*, 206. (d) Onuki, J.; Teixeira, P. C.; Medeiros, M. H. G.; Dornemann, D.; Douki, T.; Cadet, J.; Di Mascio, P. *Cell. Mol. Biol.* **2002**, *48*, 17.
- (11) (a) *SimFonia* simulation program; Shareware, Bruker, 1996. Program QPOW: (b) Belford, R. L.; Nilges, M. J. *Computer Simulation of Powder Spectra*; EPR Symposium, 21st Rocky Mountain Conference, Denver, Colorado, August 1979. (c) Nilges, M. J. Ph.D. Thesis, University of Illinois, Urbana, Illinois, 1979. (d) Cornelius, J. B.; McCracken, J.; Clarkson, R. B.; Belford, R. L.; Peisach, J. *J. Phys. Chem.* **1990**, *94*, 6977.
- (12) Stephens, B. G.; Felkel, Jr., H. L.; Spinelli, W. M. *Anal. Chem.* **1974**, *46*, 692.
- (13) (a) Valko, M.; Morris, H.; Mazur, M.; Telser, J.; McInnes, E.; Mabbs, F. *J. Phys. Chem. B* **1999**, *103*, 5591. (b) Valko, M.; Klement, R.; Pelikán, P.; Boca, R.; Dhan, L.; Böttcher, A.; Elias, H.; Müller, L. *J. Phys. Chem.* **1995**, *99*, 137. (c) Boymel, P. M.; Eaton, G. R.; Eaton, S. S. *Inorg. Chem.* **1980**, *19*, 727. (d) More, K. M.; Eaton, G. R.; Eaton, S. S. *Inorg. Chem.* **1979**, *18*, 2492. (e) Antholine, W. E.; Basosi, R.; Hyde, J. S.; Lyman, S.; Petering, D. H. *Inorg. Chem.* **1984**, *23*, 3543.
- (14) Frankel, L. S. *Chem. Commun.* **1969**, 1254.
- (15) Peisach, J.; Blumberg, W. E. *Arch. Biochem. Biophys.* **1974**, *165*, 691.
- (16) (a) Levason, W.; Spicer, M. D. *Coord. Chem. Rev.* **1987**, *76*, 45. (b) Goldstein, S.; Czapski, G.; Meyerstein, D. *J. Am. Chem. Soc.* **1990**, *112*, 6489. (c) Lamour, E.; Routier, S.; Bernier, J.-L.; Catteau, J.-P.; Bailly, C.; Vezin, H. *J. Am. Chem. Soc.* **1999**, *121*, 1862.
- (17) (a) Hanss, J.; Kruger, H. *J. Angew. Chem., Intl. Ed. Engl.* **1996**, *35*, 2827. (b) Coucouvanis, D.; Kanodia, S.; Swenson, D.; Chen, S. J.; Studemann, T.; Baenziger, N. C.; Pedelty, R.; Chu, M. *J. Am. Chem. Soc.* **1993**, *115*, 11271. (c) Bereman, R. D.; Chung, G. W.; Knight, B. W.; Singh, P.; Welch, T. W. *J. Coord. Chem.* **1994**, *32*, 51. (d) Melnik, M.; Kubesova, M. *J. Coord. Chem.* **2000**, *50*, 323.
- (18) Wu, C.-H.; Sun, L.; Faust, B. C. *J. Phys. Chem. A* **2000**, *104*, 4989.
- (19) Dodds, H. M.; Craik, D. J.; Rivory, L. P. *J. Pharm. Sci.* **1997**, *86*, 1410.
- (20) DMPO: (a) Buettner, G. R. *Free Radical Res. Commun.* **1993**, *19*, S79. (b) Buettner, G. R. *Free Radical Biol. Med.* **1987**, *3*, 259. Nitrosodurene: (c) Rehorek, D.; Janzen, E. G. *Can. J. Chem.* **1984**, *62*, 1598. (d) Sima, J.; Brezova, V. *Monatsh. Chem.* **2001**, *132*, 1493. 2,2,6,6-Tetramethyl-4-piperidinol: (e) Lion, Y.; Demelle, M.; Van De Vorst, A. *Nature (London)* **1976**, *263*, 442. (f) Moan, J.; Wold, E. *Nature (London)* **1979**, *279*, 450. (g) Inbaraj, J. J.; Gandhidasan, R.; Subramanian, S.; Murugesan, R. *J. Photochem. Photobiol., A* **1998**, *117*, 21.
- (21) (a) Li, A. S. W.; Cummings, K. B.; Roethling, H. P.; Buettner, G. R.; Chignell, C. F. *J. Magn. Reson.* **1988**, *79*, 140. The database is available through the Internet at <http://epr.niehs.nih.gov/>. (b) Janzen, E. G.; Liu, J. P. *J. Magn. Reson.* **1973**, *9*, 513. (c) Li, A. S. W.; Chignell, C. F. *J. Biochem. Biophys. Methods* **1991**, *22*, 83. (d) Bilski, P.; Chignell, C. F.; Szychliński, J.; Borkowski, A.; Oleksy, E.; Reszka, K. *J. Am. Chem. Soc.* **1992**, *114*, 549. (e) Chignell, C. F.; Motten, A. G.; Sik, R. H.; Parker, C. E.; Reszka, K. *Photochem. Photobiol.* **1994**, *59*, 5. (f) Noda, H.; Oikawa, K.; Ohya-Nishigushi, H.; Kamada, H. *Bull. Chem. Soc. Jpn.* **1993**, *66*, 3542. (g) Yoshimura, Y.; Inomata, T.; Nakazawa, H. *J. Liq. Chromatogr. Relat. Technol.* **1999**, *22*, 419. (h) Stoyanovsky, D. A.; Clancy, R.; Cederbaum, A. I. *J. Am. Chem. Soc.* **1999**, *121*, 5093. (i) Stoyanovsky, D. A.; Melnikov, Z.; Cederbaum, A. I. *Anal. Chem.* **1999**, *71*, 715. (j) Staško, A.; Raptá, P.; Brezová, V.; Nuyken, O.; Vogel, R. *Tetrahedron* **1993**, *49*, 10917.
- (22) (a) Klein, S. M.; Cohen, G.; Cederbaum, A. I. *Biochemistry* **1981**, *20*, 6006. (b) Eberhardt, K. M.; Colina, R. *J. Org. Chem.* **1988**, *53*, 1071. (c) Steiner, M. G.; Babbs, C. F. *Arch. Biochem. Biophys.* **1990**, *278*, 478. (d) Woodward, J. R.; Lin, T.-S.; Sakaguchi, Y.; Hayashi, H. *J. Phys. Chem. A* **2000**, *104*, 557. (e) Meissner, G.; Henglein, A.; Beck, G. Z. *Naturforsch., B: Chem. Sci.* **1967**, *22*, 13. (f) Veltwisch, D.; Janata, E.; Asmus, K.-D. *J. Chem. Soc., Perkin Trans. 2* **1980**, 146.
- (23) (a) Rojas Wahl, R. U.; Zeng, L.; Madison, S. A.; DePinto, R. J.; Shay, B. J. *J. Chem. Soc., Perkin Trans. 2* **1998**, 2009. (b) Dikalov, S. I.; Mason, R. P. *Free Radical Biol. Med.* **1999**, *27*, 864. (c) Ho, W. F.; Gilbert, B. C.; Davies, M. J. *J. Chem. Soc., Perkin Trans. 2* **1997**, 2525.
- (24) (a) Bilski, P.; Reszka, K.; Bilski, P.; Chignell, C. F. *J. Am. Chem. Soc.* **1996**, *118*, 1330. (b) Taniguchi, H.; Madden, K. P. *J. Phys. Chem. A* **1998**, *102*, 6753. (c) Hill, H. A. O.; Thornalley, P. J. *Inorg. Chim. Acta* **1982**, *67*, L35.
- (25) (a) Bernofsky, C.; Bandara, B. M.; Hinojosa, O. *Free Radical Biol. Med.* **1990**, *8*, 231. (b) Leonard, S.; Gannett, P. M.; Rojanasakul, Y.; Schwegler-Berry, D.; Cranston, V.; Vallyathan, V.; Shi, X. *J. Inorg. Biochem.* **1998**, *70*, 239.
- (26) Makino, K.; Hagiwara, T.; Imaishi, H.; Nishi, M.; Fujii, S.; Ohya, H.; Murakami, A. *Free Radial Res. Commun.* **1990**, *9*, 233.
- (27) (a) Reszka, K.; Bilski, P.; Sik, R. H.; Chignell, C. F. *Free Radical Res. Commun.* **1993**, *19*, S33. (b) Calle, P.; Fernández-Arizpe, A.; Sieiro, C. *Appl. Spectrosc.* **1996**, *50*, 1446. (c) Inbaraj, J. J.; Gandhidasan, R.; Murugesan, R. *J. Photochem. Photobiol., A* **1999**, *124*, 95. (d) Wu, T.; Shen, J.; Song, A.; Chen, S.; Zhang, M.; Shen, T. *J. Photochem. Photobiol., B* **2000**, *57*, 14. (e) Zhang, H.; Joseph, J.; Vazquez-Vivar, J.; Karoui, H.; Nsanumuhire, C.; Martásek, P.; Tordo, P.; Kalyanaraman, B. *FEBS Lett.* **2000**, *473*, 58. (f) Brezová, V.; Gügel, A.; Raptá, P.; Stasko, A. *J. Phys. Chem.* **1996**, *100*, 16232.
- (28) (a) Turro, N. J. *Modern Molecular Photochemistry*; University Science Books: Mill Valley, CA, 1991. (b) Michl, J.; Bonačić-Koutecký, V. *Electronic Aspects of Organic Photochemistry*; Wiley: New York, 1990. (c) Regan, J. D.; Parrish, J. A. In *The Science of Photomedicine*; Plenum Publishing: New York, 1982.
- (29) Halliwell, B.; Gutteridge, J. M. C. *Free Radicals in Biology and Medicine*, 3rd ed.; Oxford University Press: New York, 1999.
- (30) (a) Kawanishi, S.; Hiraku, Y.; Murata, M.; Oikawa, S. *Free Radical Biol. Med.* **2002**, *32*, 822. (b) Halliwell, B.; Clement, M. V.; Long, L. H. *FEBS Lett.* **2000**, *486*, 10.
- (31) (a) *Photodynamic Therapy: Basic Principles and Clinical Applications*; Henderson, B. W., Dougherty, T. J., Eds. Marcel Dekker: New York, 1992. (b) *Photodynamic Tumor Therapy*; Moser, J. G., Ed.; Gordon & Breach: Langhorne, PA, 1998. For inorganic PDT therapy, see (c) Stochel, G.; Wanat, A.; Kulis, E.; Stasicka, Z. *Coord. Chem. Rev.* **1998**, *171*, 203.
- (32) (a) Kalka, K.; Merk, H.; Mukhtar, H. *J. Am. Acad. Dermatol.* **2000**, *42*, 389. (b) Morgan, J.; Whitaker, J. E.; Oseroff, A. R. *Photochem. Photobiol.* **1998**, *67*, 155. (c) Ceburkov, O.; Gollnick, H. *Eur. J. Dermatol.* **2000**, *10*, 568. (d) Wolfen, H. C. *Endoscopy* **2000**, *32*, 715. (e) Pervais, S. *FASEB J.* **2001**, *15*, 612. (f) Barr, H.; Dix, A. J.; Kendall, C.; Stone, N. *Aliment. Pharmacol.* **2001**, *15*, 311. (g) Korbelik, M.; Sun, J. *Int. J. Cancer* **2001**, *93*, 26.